

Balancing intermolecular hydrogen-bond interactions for the directed assembly of binary 1 : 1 co-crystals

Christer B. Aakeröy,^{*a} Nate Schultheiss,^a John Desper^a and Curtis Moore^b

Received (in Montpellier, France) 12th June 2006, Accepted 12th July 2006

First published as an Advance Article on the web 25th August 2006

DOI: 10.1039/b608267j

The synthesis of three supramolecular reactants (SR's) containing two distinct hydrogen bonding donor/acceptor sites (pyridine–aminopyrimidine) designed to establish competitive intermolecular interactions during co-crystal assembly is described. These ditopic SR's were allowed to react with aromatic carboxylic acids in varied stoichiometric ratios, producing nine molecular 1 : 1 co-crystals. Single crystal X-ray diffraction studies show that in each case, the participating carboxylic acid preferentially engages in heteromeric O–H...N/N–H...O hydrogen bonds with the aminopyrimidine binding site. The results can be rationalized through a hierarchical view of intermolecular interactions based upon observed structural pattern preferences, and they also establish the reliability of the aminopyrimidine as an effective supramolecular tool, even in the presence of other potential disruptive hydrogen-bonding donor/acceptor moieties.

Introduction

The deliberate assembly of molecular building-blocks into discrete supermolecules or extended networks with predetermined stoichiometries or connectivities through non-covalent intermolecular interactions is a central challenge in the field of crystal engineering.¹ Since the individual components making up the supermolecules are brought together and organized through reversible interactions, product formation and isolation are typically required to take place in a one-pot reaction. This represents an inherent synthetic limitation in many areas of supramolecular assembly, but this problem may be overcome by identifying or establishing a hierarchy of intermolecular interactions which, in turn, may facilitate modular supramolecular synthesis.

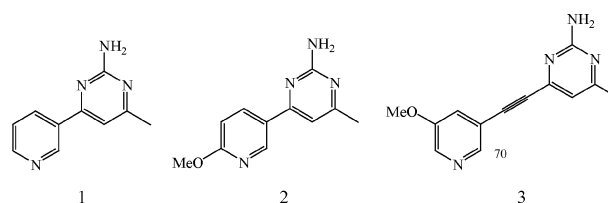
In the construction of inorganic–organic hybrid materials, it is possible to utilize one or both of the following: (1) the preferred coordination geometry of a specific metal ion and (2) the positioning and number of donor atoms on the organic ligand.² When it comes to the assembly of purely organic supramolecular architectures, synthetic strategies including, but not limited to, hydrogen bonding,³ halogen bonding,⁴ π – π stacking,⁵ have typically been employed. The hydrogen bond is a particularly powerful tool due to its strength and directionality, but it can also be fine-tuned electronically and geometrically.⁶

Etter suggested⁷ that in a system with multiple (and potentially competitive) hydrogen-bond donors and acceptors, the best hydrogen-bond donor will interact with the best hydrogen-bond acceptor, and the second-best donor will interact with the second-best acceptor and so forth. To further develop

this idea into versatile and reliable synthetic strategies for the construction of co-crystals, we have examined the structural reactivity and behavior of a family of new supramolecular reactants (SR's) containing two competing and tunable hydrogen-bonding sites. Three structurally similar pyridine–aminopyrimidine (py–pym) SR's **1–3** have been synthesized, Scheme 1. In each case, one end of the molecule contains a pyridine or methoxy-substituted pyridine moiety while the other end contains an aminopyrimidine functionality.

Correlations between the chemical nature of the donor/acceptor, and the resulting hydrogen-bond behavior have been examined extensively. For example, a systematic IR study of a series of carboxylic acid...pyridine complexes (in chloroform) show that even the weakest acid in this sequence, acetic acid, forms a 1 : 1 complex with pyridine held together by a short O–H...N hydrogen bond.⁸ The potential energy of this hydrogen bond is described by a highly asymmetrical double-minimum curve. With increasing acidity the O–H...N hydrogen bond becomes stronger and the potential energy curve has a more symmetric appearance. For intermolecular interactions of this type, correct qualitative interpretations and trends within related chemical systems can frequently be extracted from a relatively simple electrostatic description of the hydrogen bond.⁹

Pyridine is significantly more basic than unsubstituted pyrimidine and this difference in basicity (as determined by experimental pK_a values) is also reflected in electrostatic



Scheme 1 Three bifunctional ligands each carrying two distinctly different hydrogen-bonding moieties.

^a Department of Chemistry, Kansas State University, 111 Willard Hall, Manhattan, KS, USA. E-mail: aakeroy@ksu.edu; Fax: 785 532 6666; Tel: 785 532 6665

^b Department of Chemistry, Wichita State University, 1845 Fairmount, Wichita, KS, USA. Fax: 316 978 3431; Tel: 316 978 3120

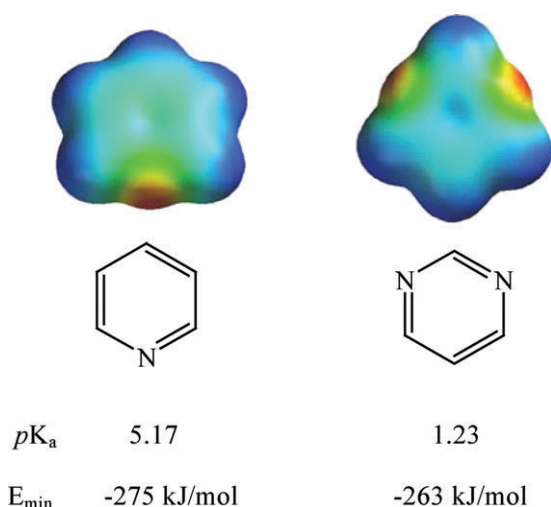


Fig. 1 Pyridine and pyrimidine and their experimental pK_a values¹⁰ and AM1 calculated electrostatic potential surfaces.¹¹

potential surfaces that can be obtained from, for example, AM1-calculations, Fig. 1.

Based on an electrostatic argument pyridine is expected to form significantly stronger $N \cdots H-O$ hydrogen bonds with an incoming carboxylic acid than is pyrimidine. There is, in fact, only one reported co-crystal that has been constructed using an $O-H \cdots N$ hydrogen bond between a carboxylic acid and unsubstituted pyrimidine,¹² whereas there are more than one hundred co-crystals in the CSD that have been synthesized primarily *via* a carboxylic acid \cdots py synthon.¹³ However, if the less basic nitrogen atom in pyrimidine is accompanied by a strong hydrogen-bond donor, such as an amino group, in the appropriate location, it may become a better hydrogen-bonding moiety than a pyridine nitrogen atom only supported by an adjacent C-H donor. In order to determine the balance and competition between two binding sites, aminopyrimidine and pyridine, and their abilities to attract the attention of a carboxylic acid, we report crystal structures of nine molecular co-crystals obtained from supramolecular reactions between **1–3** and a variety of aromatic carboxylic acids.

Experimental

Synthesis

All chemicals were purchased from Aldrich and used without further purification. The synthesis and characterization of 3-(2-amino-4-methylpyrimidin-6-yl)pyridine **1** and 1-(2-amino-4-methylpyrimidin-6-yl)-2-(3-methoxypyridin-5-yl)ethyne **3** are reported elsewhere.¹⁴ Melting points were determined on a Fisher-Johns melting point apparatus and are uncorrected. Compounds were prepared for infrared spectroscopic (IR) analysis as a mixture in KBr.

4-Methyl-3-(2-amino-4-methoxypyrimidin-6-yl)pyridine, 2. A mixture of 2-amino-4-chloro-6-methylpyrimidine (1.534 g, 10.73 mmol), 2-methoxy-5-pyridylboronic acid (1.90 g, 12.42 mmol), sodium carbonate (0.700 g, 6.60 mmol) *bis*(triphenyl-

phosphine)palladium(II) dichloride (180 mg, 0.256 mmol, 2.4 mol%) was added to a round bottom flask. Acetonitrile (35 mL) and water (35 mL) were added and dinitrogen bubbled through the resultant mixture for 10 min. A condenser was attached and the mixture heated at 65 °C under a dinitrogen atmosphere. The reaction was monitored by TLC and allowed to cool to room temperature on completion (24 h). A portion of the product **2** precipitated from the reaction mixture, thus the precipitate was filtered and the remaining reaction mixture worked up accordingly. The solution was diluted with ethyl acetate (150 mL), washed with water (3 \times 100 mL) then washed with saturated aqueous sodium chloride (1 \times 100 mL). The organic layer was separated and dried over magnesium sulfate. The solvent was removed on a rotary evaporator and the residue chromatographed on silica with a hexane-ethyl acetate mixture (1 : 3) as the eluant. The isolated product was then combined with the filtered portion. The tan solid, product **2**, was then recrystallized from ethanol as colorless bar shaped crystals (1.44 g, 64%). Mp: 163–165 °C; ¹H NMR (δ_H ; 400 MHz, CDCl₃): 8.74 (d, J = 2.8 Hz, 1H), 8.22 (dd, J = 8.8 Hz, J = 2.4 Hz, 1H), 6.87 (s, 1H), 6.82 (d, J = 8.8 Hz, 1H), 5.11 (s, 2H), 4.00 (s, 3H), 2.41 (s, 3H); ¹³C NMR (δ_C ; 400 MHz, CDCl₃): 168.62, 165.55, 163.14, 162.93, 146.33, 137.26, 126.51, 110.83, 106.30, 53.75, 24.13; IR (KBr): 3449, 3317, 1583, 1367, 1290, 1013.

3-(2-Amino-4-methylpyrimidin-6-yl)pyridine · 4-nitrobenzoic acid, 1a. 3-(2-Amino-4-methylpyrimidin-6-yl)pyridine (19 mg, 0.10 mmol) and 4-nitrobenzoic acid (17 mg, 0.10 mmol) were placed in a vial containing ethanol (6 mL) and heated until a clear homogeneous solution was obtained. After 4 d of slow evaporation, colorless rod-shaped crystals were obtained. Mp 188–190 °C; IR (KBr pellet) ν 3324 and 3171 cm⁻¹ (NH₂, m), 2425 and 1910 cm⁻¹ (O-H \cdots N, br), 1700 cm⁻¹ (C=O, m).

3-(2-Amino-4-methylpyrimidin-6-yl)pyridine · pentamethylbenzoic acid, 1b. 3-(2-Amino-4-methylpyrimidin-6-yl)pyridine (10 mg, 0.05 mmol) and pentamethylbenzoic acid (21 mg, 0.10 mmol) were placed in a vial containing an ethanol-ethyl acetate mixture (5 : 5 mL) and heated until a clear homogeneous solution was obtained. After 2 d of slow evaporation, yellow/orange prism-shaped crystals were obtained. Mp 155–157 °C; IR (KBr pellet) ν 3331 and 3198 cm⁻¹ (NH₂, m), 2442 and 1912 cm⁻¹ (O-H \cdots N, br), 1635 cm⁻¹ (C=O, m).

3-(2-Amino-4-methylpyrimidin-6-yl)pyridine · 4-hydroxybenzoic acid, 1c. 3-(2-Amino-4-methylpyrimidin-6-yl)pyridine (11 mg, 0.06 mmol) and 4-hydroxybenzoic acid (16 mg, 0.12 mmol) were placed in a vial containing ethanol (10 mL) and heated until a clear homogeneous solution was obtained. After 2 d of slow evaporation, yellowish/orange cube-shaped crystals were obtained. Mp 195–197 °C; IR (KBr pellet) ν 3432 (OH, s), 3314 and 3191 cm⁻¹ (NH₂, m), 2494 and 1875 cm⁻¹ (O-H \cdots N, br), 1655 cm⁻¹ (C=O, m).

4-Methoxy-3-(2-amino-4-methylpyrimidin-6-yl)pyridine · 4-N,N-dimethylaminobenzoic acid, 2a. 4-Methoxy-3-(2-amino-4-methylpyrimidin-6-yl)pyridine (10 mg, 0.05 mmol) and 4-N,N-dimethylaminobenzoic acid (8 mg, 0.05 mmol) were placed in a vial containing ethyl acetate (10 mL) and heated until a clear

homogeneous solution was obtained. After 1 d of slow evaporation, colorless cube-shaped crystals were obtained. Mp 173–175 °C; IR (KBr pellet) ν 3317 and 3204 cm^{-1} (NH_2 , m), 2455 and 1872 cm^{-1} ($\text{O}-\text{H}\cdots\text{N}$, br), 1705 cm^{-1} ($\text{C}=\text{O}$, m).

4-Methoxy-3-(2-amino-4-methylpyrimidin-6-yl)pyridine · 2,4-difluorobenzoic acid, 2b. 4-Methoxy-3-(2-amino-4-methylpyrimidin-6-yl)pyridine (10 mg, 0.05 mmol) and 2,4-difluorobenzoic acid (15 mg, 0.10 mmol) were placed in a vial containing methanol (10 mL) and heated until a clear homogeneous solution was obtained. After 2 d of slow evaporation, colorless rod-shaped crystals were obtained. Mp 165–167 °C; IR (KBr pellet) ν 3350 and 3191 cm^{-1} (NH_2 , m), 2372 and 1880 cm^{-1} ($\text{O}-\text{H}\cdots\text{N}$, br), 1685 cm^{-1} ($\text{C}=\text{O}$, m).

4-Methoxy-3-(2-amino-4-methylpyrimidin-6-yl)pyridine · pentamethylbenzoic acid, 2c. 4-Methoxy-3-(2-amino-4-methylpyrimidin-6-yl)pyridine (13 mg, 0.06 mmol) and pentamethylbenzoic acid (23 mg, 0.12 mmol) were placed in a vial containing ethanol (6 mL) and heated until a clear homogeneous solution was obtained. After 2 d of slow evaporation, colorless rod-shaped crystals were obtained. Mp 181–183 °C; IR (KBr pellet) ν 3385 and 3206 cm^{-1} (NH_2 , m), 2429 and 1926 cm^{-1} ($\text{O}-\text{H}\cdots\text{N}$, br), 1653 cm^{-1} ($\text{C}=\text{O}$, m).

1-(2-Amino-4-methylpyrimidin-6-yl)-2-(3-methoxypyridin-5-yl)ethyne · 3,5-dinitrobenzoic acid, 3a. 1-(2-Amino-4-methylpyrimidin-6-yl)-2-(3-methoxypyridin-5-yl)ethyne (10 mg, 0.04 mmol) and 3,5-dinitrobenzoic acid (9 mg, 0.04 mmol) were placed in a vial containing an ethanol–ethyl acetate mixture (15 : 15 mL) and heated until a clear homogeneous solution was obtained. After 1 d of slow evaporation, colorless plate-shaped crystals were obtained. Mp 235–237 °C; IR (KBr pellet) ν 3314 and 3145 cm^{-1} (NH_2 , m), 2479 and 1890 cm^{-1} ($\text{O}-\text{H}\cdots\text{N}$, br), 2223 cm^{-1} ($\text{C}\equiv\text{C}$), 1690 cm^{-1} ($\text{C}=\text{O}$, m).

1-(2-Amino-4-methylpyrimidin-6-yl)-2-(3-methoxypyridin-5-yl)ethyne · 4-nitrobenzoic acid, 3b. 1-(2-Amino-4-methylpyrimidin-6-yl)-2-(3-methoxypyridin-5-yl)ethyne (10 mg, 0.04 mmol) and 4-nitrobenzoic acid (14 mg, 0.08 mmol) were placed in a vial containing an ethanol–ethyl acetate mixture (10 : 10 mL) and heated until a clear homogeneous solution was obtained. After 1 d of slow evaporation, colorless plate-shaped crystals were obtained. Mp 196–198 °C; IR (KBr pellet) ν 3385 and 3304 cm^{-1} (NH_2 , m), 2428 and 1885 cm^{-1} ($\text{O}-\text{H}\cdots\text{N}$, br), 2222 cm^{-1} ($\text{C}\equiv\text{C}$), 1697 cm^{-1} ($\text{C}=\text{O}$, m).

1-(2-Amino-4-methylpyrimidin-6-yl)-2-(3-methoxypyridin-5-yl)ethyne · 3-*N,N*-dimethylaminobenzoic acid, 3c. 1-(2-Amino-4-methylpyrimidin-6-yl)-2-(3-methoxypyridin-5-yl)ethyne (12 mg, 0.06 mmol) and 3-*N,N*-dimethylaminobenzoic acid (18 mg, 0.12 mmol) were placed in a vial containing ethanol (6 mL) and heated until a clear homogeneous solution was obtained. After 3 d of slow evaporation, yellow block-shaped crystals were obtained. Mp 168–170 °C; IR (KBr pellet) ν 3324 and 3140 cm^{-1} (NH_2 , m), 2413 and 1895 cm^{-1} ($\text{O}-\text{H}\cdots\text{N}$, br), 2228 cm^{-1} ($\text{C}\equiv\text{C}$), 1655 cm^{-1} ($\text{C}=\text{O}$, m).

X-Ray crystallography

Datasets for compounds **1c**, **2a**, **2b**, **2c**, **3b**, and **3c** were collected on a SMART APEX. Data for compounds **1a**, **1b**, and **3a** were collected on a SMART 1000. All datasets were collected using Mo-K α radiation and were uncorrected for absorption, Table 1.

CCDC reference numbers 614724–614732.

For crystallographic data in CIF or other electronic format see DOI: 10.1039/b608267j

Data were collected using SMART.¹⁵ Initial cell constants were found by small widely separated “matrix” runs. An entire hemisphere of reciprocal space was collected. Scan speed and

Table 1 Crystallographic data for **1a–3c**

	1a	1b	1c	2a	2b	2c	3a	3b	3c
Formula moiety	(C ₁₀ H ₁₀ N ₄) (C ₇ H ₅ NO ₄)	(C ₁₀ H ₁₀ N ₄) (C ₁₂ H ₁₆ O ₂)	(C ₁₀ H ₁₀ N ₄) (C ₇ H ₆ O ₃)	(C ₁₁ H ₁₂ N ₄ O) (C ₉ H ₁₁ O ₂)	(C ₁₁ H ₁₂ N ₄ O) (C ₁₂ H ₁₆ O ₂)	(C ₁₁ H ₁₂ N ₄ O) (C ₇ H ₄ F ₂ O ₂)	(C ₁₃ H ₁₂ N ₄ O) (C ₇ H ₄ N ₂ O ₆)	(C ₁₃ H ₁₂ N ₄ O) (C ₇ H ₅ NO ₄)	(C ₁₃ H ₁₂ N ₄ O) (C ₉ H ₁₁ NO ₂)
Formula weight	353.34	378.47	324.34	381.43	408.49	374.35	452.39	407.39	405.45
Crystal system	Triclinic	Triclinic	Triclinic	Triclinic	Triclinic	Monoclinic	Triclinic	Triclinic	Monoclinic
Space group, <i>Z</i>	<i>P</i> 1, 2	<i>P</i> 1, 2	<i>P</i> 1, 2	<i>P</i> 1, 2	<i>P</i> 1, 2	<i>C</i> 2/ <i>c</i> , 8	<i>P</i> 1, 2	<i>P</i> 1, 2	<i>P</i> 2(1)/ <i>c</i> , 4
<i>a</i> /Å	6.8245(5)	8.2088(7)	8.3089(6)	7.8442(12)	5.3534(5)	33.158(4)	7.374(11)	6.9157(12)	10.5742(19)
<i>b</i> /Å	9.5538(7)	8.7891(6)	8.9991(7)	8.8879(14)	12.6941(12)	7.3848(7)	8.385(13)	6.9405(12)	14.599(3)
<i>c</i> /Å	12.6278(9)	15.3371(12)	11.1671(7)	14.216(2)	15.1880(14)	14.1634(16)	17.56(3)	19.854(4)	13.519(3)
α /°	77.174(4)	92.767(5)	86.733(4)	101.607(2)	87.7550(10)	90	93.51(10)	87.646(3)	90
β /°	84.400(4)	105.536(4)	69.174(4)	90.830(2)	82.9210(10)	106.439(6)	96.29(7)	80.636(3)	102.453(11)
γ /°	82.637(4)	115.332(4)	77.699(5)	106.753(2)	87.542(2)	90	105.50(11)	81.138(3)	90
Volume/Å ³	794.13(10)	946.59(13)	762.52(9)	926.8(2)	1022.72(17)	3326.4(6)	1040(3)	928.9(3)	2037.9(7)
Temperature/K	173(2)	173(2)	153(2)	100(2)	100(2)	293(2)	173(2)	100(2)	293(2)
Density/g cm ^{−3}	1.478	1.328	1.413	1.367	1.327	1.495	1.444	1.457	1.322
X-Ray wavelength	0.71073	0.71073	0.71073	0.71073	0.71073	0.71073	0.71073	0.71073	0.71073
μ/mm^{-1}	0.109	0.087	0.100	0.095	0.090	0.119	0.113	0.108	0.091
$\theta_{\text{min}}/\text{°}$	2.46	1.40	1.95	2.45	2.06	2.56	2.34	2.08	2.42
$\theta_{\text{max}}/\text{°}$	28.27	27.90	26.43	28.30	28.31	27.18	27.14	26.02	27.22
Reflections									
Collected	5974	6992	22047	8262	8494	68430	7011	4809	44586
Independent	3581	4181	3129	4281	4648	3690	4228	3438	4534
Observed	2272	4048	1979	3502	3490	1598	1209	2099	2037
Threshold expression	$> 2\sigma(I)$	$> 2\sigma(I)$	$> 2\sigma(I)$	$> 2\sigma(I)$	$> 2\sigma(I)$	$> 2\sigma(I)$	$> 2\sigma(I)$	$> 2\sigma(I)$	$> 2\sigma(I)$
<i>R</i> 1 (observed)	0.0506	0.0738	0.0863	0.0458	0.0519	0.0558	0.1139	0.0532	0.0773
<i>wR</i> 2 (all)	0.1485	0.2100	0.2161	0.1318	0.1483	0.1514	0.3299	0.1382	0.2304

scan width were chosen based on scattering power and peak rocking curves.

Unit cell constants and orientation matrix were improved by least-squares refinement of reflections thresholded from the entire dataset. Integration was performed with SAINT,¹⁶ using this improved unit cell as a starting point. Precise unit cell constants were calculated in SAINT from the final merged dataset. Lorenz and polarization corrections were applied, and data were corrected for absorption.

Data were reduced with SHELXTL.¹⁷ All structures were solved by direct methods. In general, hydrogen atoms were assigned to idealized positions and were allowed to ride. Where possible, the coordinates of hydrogen-bonding hydrogens were allowed to refine. Where appropriate, weighting schemes were optimized based on the recommendations from SHELXL. Heavy atoms were refined with anisotropic thermal parameters. For all structures *except* **3a**,¹⁸ positional coordinates for carboxylic acid hydrogens (labelled H31 except for **2c**, where it is labelled H41) and amine hydrogens (H12A and H12B for all structures) were allowed to refine. Coordinates for the phenolic hydrogen atom H34 of **1c** were allowed to refine.

Results and discussion

The primary motif in the crystal structure of **1a** is composed of one ligand **1** and one 4-nitrobenzoic acid molecule connected through the acid and aminopyrimidine moieties, Fig. 2. The primary synthons are O–H...N and N–H...O hydrogen bonds with O31...N11 and N12...O32 distances of 2.5274(18) and

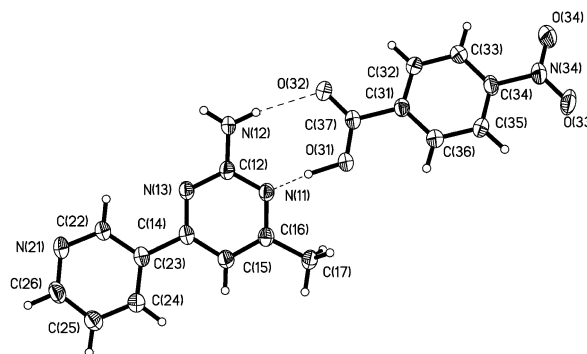


Fig. 2 Thermal-ellipsoids plot (50% probability level) of the 1 : 1 binary co-crystal of **1a**.

3.034(2) Å, respectively, Table 2. Secondary N–H...N hydrogen bonds, N12...N21, 3.015(2) Å, formed from the *anti*-amino proton and the pyridyl nitrogen atom extend the architecture into a four-component supermolecule, Fig. 3.

The primary motif in the crystal structure of **1b** contains one ligand **1** and one pentamethylbenzoic acid molecule, interconnected through the acid and aminopyrimidine moieties, Fig. 4. The primary synthons are O–H...N and N–H...O hydrogen bonds with O41...N11 and N12...O42 distances of 2.599(2) and 3.013(2) Å, respectively. Secondary N–H...N hydrogen bonds, N12...N21, 3.112(3) Å, between the *anti*-amino proton and the pyridyl nitrogen atom extend the architecture into a one-dimensional strand, Fig. 5.

Table 2 Hydrogen-bond geometries for **1a–3c**

Co-crystal	D–H...H	<i>d</i> (D–H)/Å	<i>d</i> (H...A)/Å	<i>d</i> (D...A)/Å	∠(DHA)/°
1a^a	N(12)–H(12B)...O(32)	0.90(2)	2.14(2)	3.034(2)	170.9(19)
	N(12)–H(12A)...N(21)#1	0.87(2)	2.14(2)	3.015(2)	177.4(19)
	O(31)–H(31)...N(11)	1.17(2)	1.36(2)	2.5274(18)	174.4(19)
1b^b	O(41)–H(41)...N(11)	0.90(3)	1.72(3)	2.599(2)	164(3)
	N(12)–H(12A)...O(42)	0.87(3)	2.15(3)	3.013(2)	176(3)
	N(12)–H(12B)...N(21)#1	0.88(3)	2.46(3)	3.112(3)	132(2)
1c^c	N(12)–H(12A)...O(32)	0.83(4)	2.08(4)	2.906(3)	170(3)
	N(12)–H(12B)...O(34) #1	0.93(3)	2.28(4)	157(3)	3.163(3)
	O(31)–H(31)...N(11)	0.91(4)	1.75(4)	2.656(3)	173(3)
2a^d	O(34)–H(34)...N(21)#2	0.93(3)	1.80(4)	2.728(3)	169(3)
	O(31)–H(31)...N(11)	0.951(17)	1.690(17)	2.6321(14)	170.0(15)
	N(12)–H(12A)...O(32)	0.894(17)	2.026(17)	2.9173(15)	174.3(14)
2b^e	N(12)–H(12B)...O(32)#1	0.862(16)	2.110(16)	2.8925(15)	150.8(14)
	N(12)–H(12A)...O(32)	0.92(3)	2.02(3)	2.925(3)	170(2)
	N(12)–H(12B)...N(11)#1	0.94(3)	2.16(3)	3.085(3)	172(2)
2c^f	O(31)–H(31)...N(13)	0.91(3)	1.70(3)	2.604(3)	174(3)
	N(12)–H(12A)...O(42)	0.91(2)	2.05(2)	2.9519(19)	173.1(19)
	N(12)–H(12B)...N(21)#1	0.85(2)	2.25(2)	3.080(2)	165.3(19)
3a^g	O(41)–H(41)...N(11)	0.90(2)	1.77(2)	2.6515(18)	167(2)
	–(12)–H(12A)...O(32)	0.88	2.19	3.049(9)	165.6
	N(12)–H(12B)...N(13)#1	0.88	2.24	3.121(12)	175.3
3b^h	O(31)–H(31)...N(11)	0.84	1.84	2.633(9)	157.2
	N(12)–H(12A)...O(32)	0.91(3)	2.22(3)	3.109(3)	168(2)
	O(31)–H(31)...N(11)	0.99(3)	1.67(3)	2.652(3)	173(3)
3cⁱ	N(12)–H(12B)...N(13)#1	0.90(3)	2.24(3)	3.122(3)	168(2)
	O(31)–H(31)...N(11)	0.96(4)	1.67(4)	2.625(3)	170(3)
	N(12)–H(12A)...O(32)	0.99(3)	1.92(3)	2.908(4)	177(3)
	N(12)–H(12B)...N(21)#1	0.95(3)	2.09(3)	3.023(4)	171(3)

^a #1 –x, –y, –z + 1. ^b #1 x + 1, y + 1, z. ^c #1 x, y, z – 1 #2 x + 1, y – 1, z + 1. ^d #1 –x + 1, –y + 1, –z + 1. ^e #1 –x + 1, y, –z + 1/2.

^f #1 –x + 1, –y + 2, –z + 1. ^g #1 –x + 2, –y + 1, –z + 1. ^h #1 –x + 1, –y, –z + 1. ⁱ #1 –x, y – 1/2, –z + 1/2.

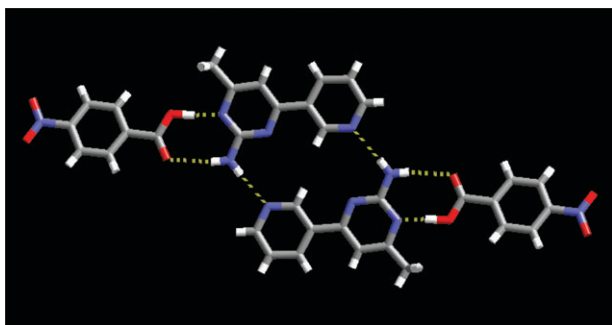


Fig. 3 A four-component supermolecule in **1a** formed through multiple O–H...N, N–H...O and N–H...N hydrogen bonds.

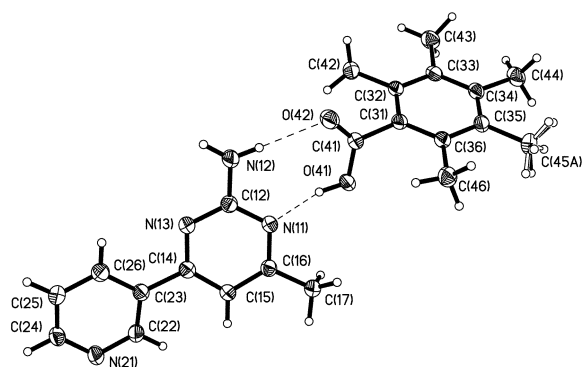


Fig. 4 Thermal-ellipsoids plot (50% probability level) of the 1 : 1 binary co-crystal of **1b**.

In the crystal structure of **1c** the main motif consists of one ligand **1** and one 4-hydroxybenzoic acid molecule, assembled via a complementary hydrogen-bond interaction between the carboxylic acid and the aminopyrimidine moiety, Fig. 6. The primary hydrogen bonds are O–H...N and N–H...O interactions



Fig. 5 1-D strand formed through secondary N–H...N hydrogen bonds from 1 : 1 ligand : acid dimers of **1b**.

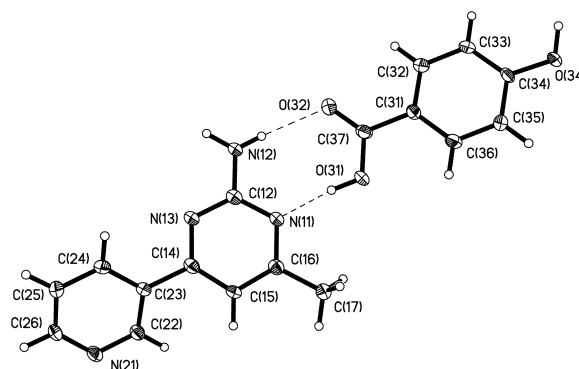


Fig. 6 Thermal-ellipsoids plot (50% probability level) of the 1 : 1 binary co-crystal of **1c**.

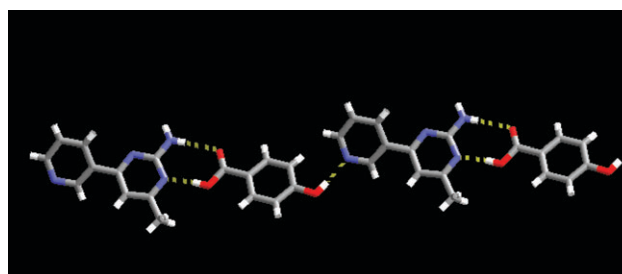


Fig. 7 Infinite one-dimensional chain formed through acid-aminopyrimidine and hydroxy...pyridine hydrogen bonds in **1c**.

with O31...N11 and N12...O32 distances of 2.656(3) and 2.906(3) Å, respectively. Secondary O–H...N hydrogen bonds, O34...N21, 2.728(3) Å, formed through the hydroxyl proton and the pyridyl nitrogen atom extend the architecture into a one-dimensional chain, Fig. 7.

The primary supermolecule in the crystal structure of **2a** consists of one ligand **2** and one 4-*N,N*-dimethylaminobenzoic acid molecule; the two molecules are again connected through the acid and aminopyrimidine moieties, Fig. 8. The primary

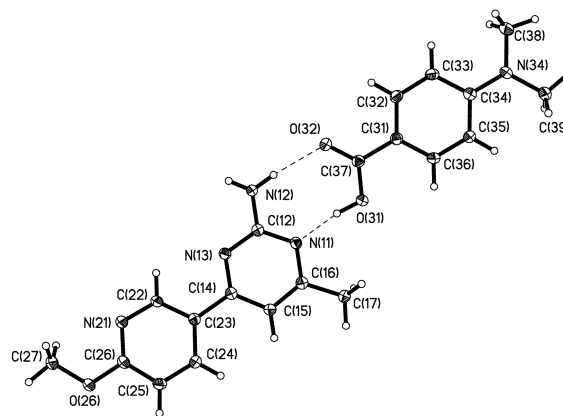


Fig. 8 Thermal-ellipsoids plot (50% probability level) of the 1 : 1 binary co-crystal of **2a**.

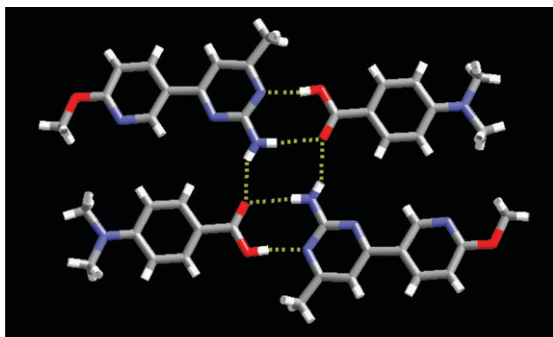


Fig. 9 Four-component supermolecule in **2a** formed through a series of O–H···N and N–H···O hydrogen bonds.

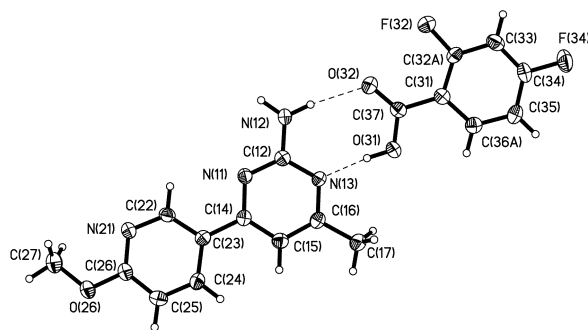


Fig. 10 Thermal-ellipsoids plot (50% probability level) of the 1 : 1 binary co-crystal of **2b**.

synthons in this structure are O—H...N and N—H...O hydrogen bonds with O31...N11 and N12...O32 distances of 2.6321(14) and 2.9173(15) Å, respectively. Secondary N—H...O hydrogen bonds, N12...O32, 2.8925(15) Å, formed from the *anti*-amino proton and the carboxylic acid oxygen atom extend the structure into a four-component supermolecule, Fig. 9.

In the crystal structure of **2b**, one ligand **2** and one 2,4-difluorobenzoic acid molecule form the primary hydrogen bonds between the carboxylic acid and aminopyrimidine moieties, Fig. 10. The primary synthons in this structure are O–H...N and N–H...O hydrogen bonds with O31...N13 and

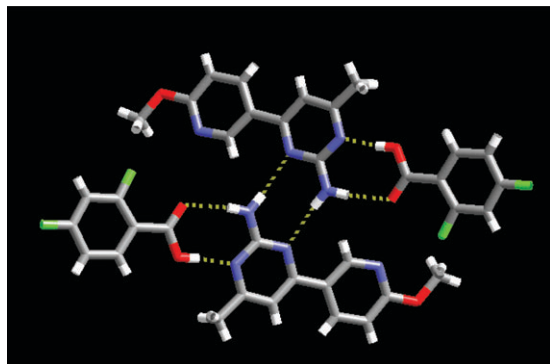


Fig. 11 Tetrameric supermolecule in **2b** formed through a series of O–H···N, N–H···O and N–H···N hydrogen bonds.

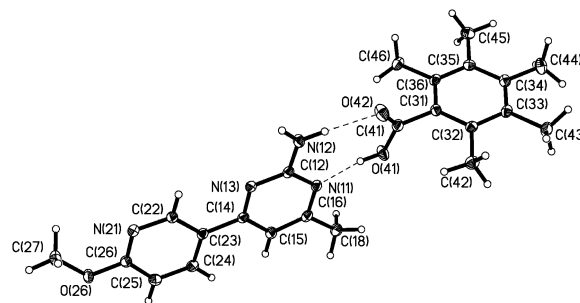


Fig. 12 Thermal-ellipsoids plot (50% probability level) of the 1 : 1 binary co-crystal of **2c**.

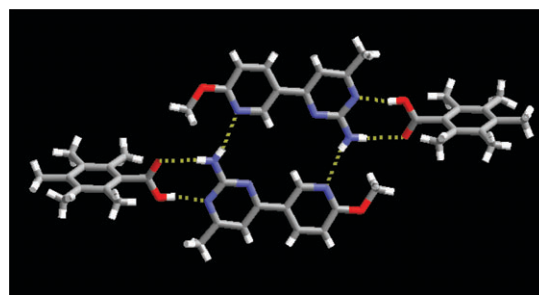


Fig. 13 Four-component supermolecule in **2c** formed through a series of O–H...N, N–H...O and N–H...N hydrogen bonds.

N12...O32 distances of 2.604(3) and 2.925(3) Å, respectively. Secondary N—H...N hydrogen bonds, N12...N11, 3.085(3) Å, between the *anti*-amino proton and the second pyrimidine nitrogen atom lead to a four-component supermolecule, Fig. 11.

The 1 : 1 co-crystal of **2c** shows a primary motif composed of **2** and one pentamethylbenzoic acid molecule, which are interlinked through the carboxylic acid and the aminopyrimidine moieties, Fig. 12. The primary synthons in this structure are O—H...N and N—H...O hydrogen bonds with O41...N11

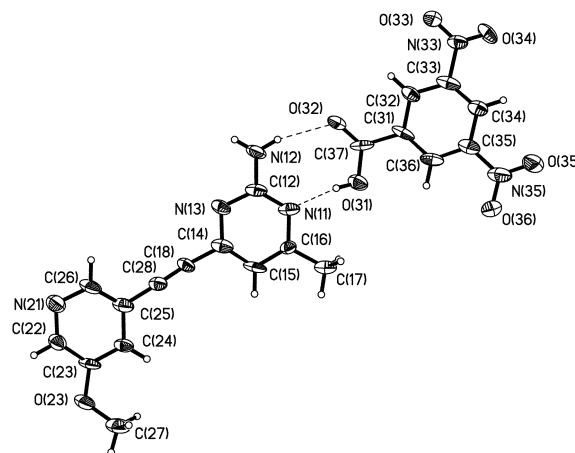


Fig. 14 Thermal-ellipsoids plot (50% probability level) of the 1 : 1 binary co-crystal of **3a**.

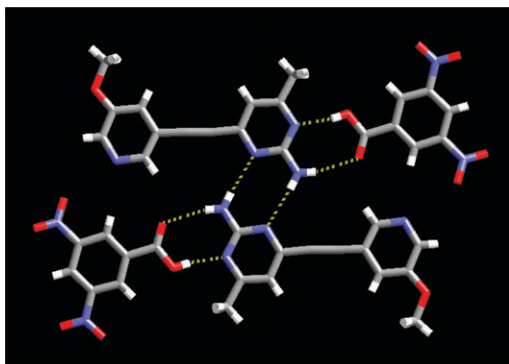


Fig. 15 Four-component supermolecule in **3a** formed through O–H...N, N–H...O and N–H...N hydrogen bonds.

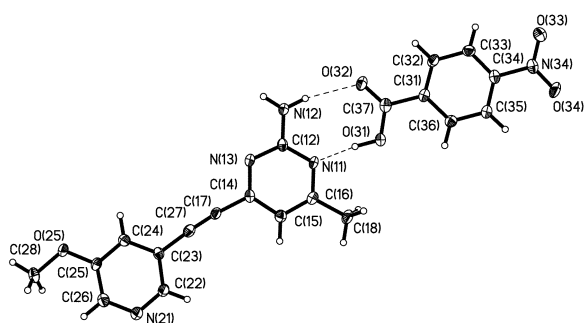


Fig. 16 Thermal-ellipsoids plot (50% probability level) of the 1 : 1 binary co-crystal of **3b**.

and N12...O34 distances of 2.6515(18) and 2.9519(19) Å, respectively. Secondary N–H...N hydrogen bonds, N12...N21, 3.080(2) Å, between the *anti*-amino proton and the pyridyl nitrogen atom extend the architecture into a four-component supermolecule, Fig. 13.

The central motif in the crystal structure of **3a** contains **3** and one 3,5-dinitrobenzoic acid molecule, constructed with complementary hydrogen bonds between the carboxylic acid and the aminopyrimidine moiety, Fig. 14. The primary synthons in this structure are O–H...N and N–H...O hydrogen bonds with O31...N11 and N12...O32 distances of 2.633(9)

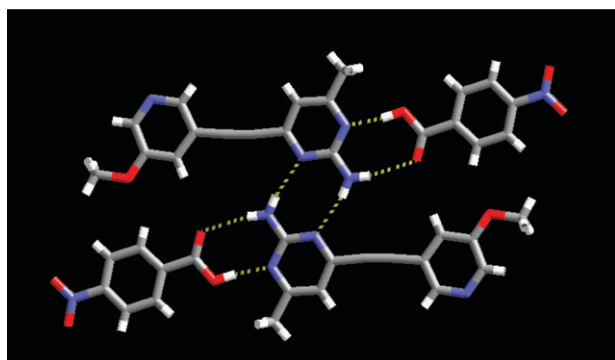


Fig. 17 Four-component supermolecule in **3b** formed through a series of O–H...N, N–H...O and N–H...N hydrogen bonds.

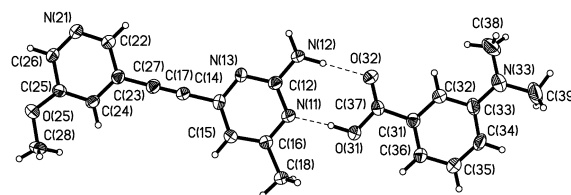


Fig. 18 Thermal-ellipsoids plot (50% probability level) of the 1 : 1 binary co-crystal of **3c**.

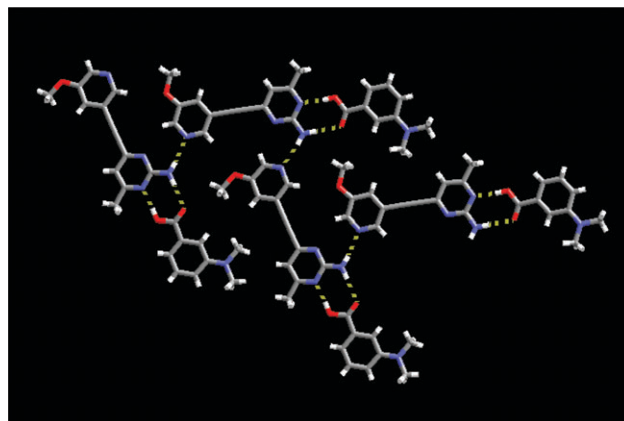


Fig. 19 1-D strand in **3c** formed through secondary N–H...N hydrogen bonds between the *anti*-amino proton and the pyridine nitrogen atom.

and 3.049(9) Å, respectively. Secondary N–H...N hydrogen bonds, N12...N13, 3.121(12) Å, between the *anti*-amino proton and second pyrimidine nitrogen atom extend the structure into a four-component supermolecule, Fig. 15.

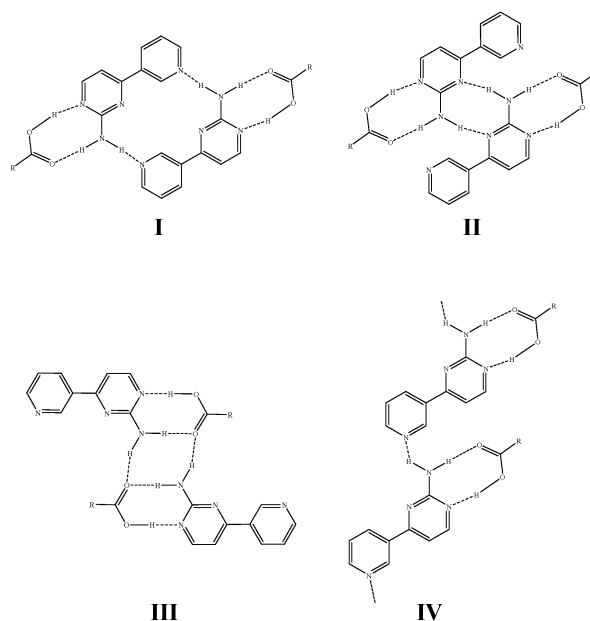
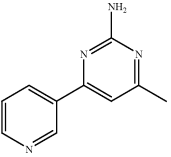
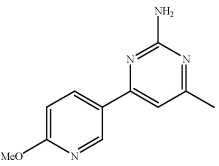
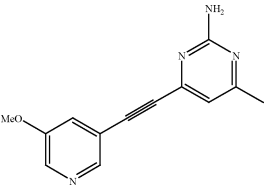


Fig. 20 Observed motifs between supramolecular dimers in co-crystals obtained from reactions between SR's **1–3** and a carboxylic acid.

Table 3 Summary of secondary structural motifs

SR	Carboxylic acid	Structure	Secondary structural motif
	4-Nitrobenzoic acid	1a	I
	Pentamethylbenzoic acid	1b	IV
	4-Hydroxybenzoic acid	1c	—
	4- <i>N,N</i> -Dimethylaminobenzoic acid	2a	III
	2,4-Difluorobenzoic acid	2b	II
	Pentamethylbenzoic acid	2c	I
	3,5-Dinitrobenzoic acid	3a	II
	4-Nitrobenzoic acid	3b	II
	3- <i>N,N</i> -Dimethylaminobenzoic acid	3c	IV

The crystal structure of **3b** contains SR **3** and one 4-nitrobenzoic acid molecule that are linked through hydrogen bonds between the carboxylic acid and the aminopyrimidine moieties, Fig. 16. The primary synthons in this structure are O—H...N and N—H...O hydrogen bonds with O31...N11 and N12...O32 distances of 2.652(3) and 3.109(3) Å, respectively. Secondary N—H...N hydrogen bonds, N12...N13, 3.122(3) Å, between the *anti*-amino proton and second pyrimidine nitrogen atom extend the structure into a four-component supermolecule, Fig. 17.

Finally, the crystal structure of **3c** contains a supermolecule constructed with one ligand **3** and one 3-*N,N*-dimethylaminobenzoic acid molecule, held together with hydrogen bonds between the carboxylic acid and the aminopyrimidine site, Fig. 18. The primary synthons in this structure are O—H...N and N—H...O hydrogen bonds with O31...N11 and N12...O32 distances of 2.625(3) and 2.908(4) Å, respectively. Secondary N—H...N hydrogen bonds, N12...N21, 3.023(3) Å, between the *anti*-amino proton and pyridine nitrogen atom extend the structure into a 1-D strand, Fig. 19.

In every one of the nine co-crystals containing SR's **1–3** and a carboxylic acid that we have obtained so far, the primary intermolecular interaction responsible for the construction of the main supramolecular assembly, is a pairwise O—H...N/N—H...O motif between the carboxylic acid and the aminopyrimidine moiety.

It is possible that SR **2** did not form hydrogen bonds at the pyridyl site because the nitrogen atom is somewhat sterically hindered by the neighboring methoxy-group, potentially blocking an incoming carboxylic acid. However upon moving the methoxy-group to the *meta*-position, thereby removing any possibility of steric congestion, the approaching carboxylic acid still interacts preferentially with the aminopyrimidine moiety.

It is worth emphasizing that the py...carboxylic acid N...H—O heteromeric hydrogen-bond interaction is a very

effective tool for the deliberate assembly of molecular co-crystals,¹⁹ and a search of the CSD¹³ reveals that twenty-one co-crystals, assembled *via* complementary carboxylic acid-aminopyrimidine interactions, exist.²⁰ Clearly, both synthons are suitable supramolecular tools, capable of bringing together a variety of discrete molecular building blocks into heteromeric molecular co-crystals. The competition between the two types of synthons has not yet been examined in a systematic manner, but the structural results presented herein, clearly demonstrate that the aminopyrimidine site is much more competitive for a carboxylic acid than is a pyridine moiety. In fact, we have yet to find any exceptions to this structural behavior, which equates to a high supramolecular yield.

Beyond the primary interactions that consistently take place between the carboxylic acid and 2-aminopyrimidine (the dominating receptor in this study), we have identified four types of motifs that take place between adjacent supramolecular dimers in this series of compounds, Fig. 20.

The frequency of occurrence of each type of motif is summarized in Table 3. The crystal structure of **1c** is somewhat different because the pyridine nitrogen atom is acting as an acceptor for the O—H substituent of the carboxylic acid, which leaves the *anti*-NH₂ proton as a donor for the same hydroxyl group. However, in four out of the eight remaining structures, the *anti* proton prefers to interact with the pyridine nitrogen atom. On one occasion the pyridine nitrogen atom is engaged in a hydrogen bond with a C—H moiety located next to a nitro group (in **3a**). The pyridine site is left alone on three occasions (in **2a–b** and **3b**) with no short contacts to any C—H group.

Conclusions

The major finding reported in this study centers on the fact that we have been able to establish differences in hydrogen-bond capacity of related binding sites through a systematic

structural study of co-crystals based on custom-designed supramolecular reactants. Despite the fact that unsubstituted pyrimidine is a rather poor hydrogen-bond acceptor, and certainly not competitive with a pyridine moiety, the addition of an amino group to the former heterocycle shifts the balance very strongly in its favor as a competitive binding site for carboxylic acids.

We are currently examining if readily available calculated electrostatic potential surfaces can provide tools for determining hydrogen-bond preferences in series of related compounds which, in turn, would allow us to predict (to some extent) connectivities, stoichiometries and dimensionalities of supramolecular architectures. Systematic structural studies, such as the one presented herein, provide the essential foundation for such efforts and may eventually offer transferable, versatile and practical avenues for predictable supramolecular synthesis.

Acknowledgements

Financial support from NSF (CHE-0316479) and Kansas State University is gratefully appreciated. We also thank Dr Doug Powell (Oklahoma University) for the single-crystal data collections of **2a**, **2c**, and **3b**.

References

- (a) C. B. Aakeröy and D. J. Salmon, *CrystEngComm*, 2005, **7**, 439; (b) J. W. Steed and J. L. Atwood, *Supramolecular Chemistry*, John Wiley and Sons Ltd, Chichester, 2000; (c) J.-M. Lehn, *Supramolecular Chemistry*, VCH, Weinheim, 1995; (d) G. R. Desiraju, *Crystal Engineering The Design of Organic Solids*, Elsevier Science Publishers B.V., Amsterdam, 1989.
- (a) M. Fujita, M. Tominaga, A. Hori and B. Therrien, *Acc. Chem. Res.*, 2005, **38**, 369; (b) D. Fiedler, D. H. Leung, R. G. Bergman and K. N. Raymond, *Acc. Chem. Res.*, 2005, **38**, 349; (c) M. W. Hosseini, *Acc. Chem. Res.*, 2005, **38**, 313; (d) M. Eddaoudi, D. B. Moler, H. Li, B. Chen, T. M. Reineke, M. O'Keeffe and O. M. Yaghi, *Acc. Chem. Res.*, 2001, **34**, 319.
- (a) L. MacGillivray, *CrystEngComm*, 2004, **6**, 77; (b) J.-M. Lehn, *Science*, 2002, **295**, 2400; (c) G. R. Desiraju, *Acc. Chem. Res.*, 2002, **35**, 565; (d) B. Moulton and M. J. Zaworotko, *Chem. Rev.*, 2001, **101**, 1629; (e) G. R. Desiraju, *Angew. Chem., Int. Ed. Engl.*, 1995, **34**, 2311.
- (a) P. Metrangolo, H. Neukirch, T. Pilati and G. Resnati, *Acc. Chem. Res.*, 2005, **38**, 386; (b) P. Metrangolo, T. Pilati, G. Resnati and A. Stevenazzi, *Chem. Commun.*, 2004, 1492; (c) A. De Santis, A. Forni, R. Liantonio, P. Metrangolo, T. Pilati and G. Resnati, *Chem.-Eur. J.*, 2003, **9**, 3974; (d) R. B. Walsh, C. W. Padgett, P. Metrangolo, G. Resnati, T. W. Hanks and W. T. Pennington, *Cryst. Growth Des.*, 2001, **1**, 165.
- N. Motohiro, *CrystEngComm*, 2004, **6**, 130, and references within.
- (a) S. Varaghese and V. R. Pedireddi, *Chem.-Eur. J.*, 2006, **12**, 1597; (b) T. R. Shattock, P. Vishweshwar, Z. Wang and M. J. Zaworotko, *Cryst. Growth Des.*, 2005, **5**, 2046; (c) C. B. Aakeröy, J. Desper and J. F. Urbina, *CrystEngComm*, 2005, **7**, 193; (d) D. Braga and F. Grepioni, *Chem. Commun.*, 2005, 3635; (e) B. K. Saha, A. Nangia and M. Jaskolski, *CrystEngComm*, 2005, **7**, 355; (f) S. Basavoju and A. Nangia, *Cryst. Growth Des.*, 2005, **5**, 1683; (g) C. B. Aakeröy, A. M. Beatty and B. A. Helfrich, *J. Am. Chem. Soc.*, 2002, **124**, 14425.
- (a) M. C. Etter, *Acc. Chem. Res.*, 1990, **23**, 120; (b) M. C. Etter, *J. Phys. Chem.*, 1991, **95**, 4601.
- R. Langner and C. J. Zundel, *J. Chem. Soc., Faraday Trans.*, 1995, **91**, 3831.
- (a) C. A. Hunter, *Angew. Chem., Int. Ed.*, 2004, **43**, 5310; (b) M. Henry and M. W. Hosseini, *New J. Chem.*, 2004, **28**, 897.
- Dissociation constants of organic bases in aqueous solutions*, ed. D. D. Perrin, International Union of Pure and Applied Chemistry, Butterworths, London, 1965.
- Molecular structures were constructed using Spartan '04 (Wavefunction, Inc. Irvine, CA), and their geometries were optimized using AM1, with the maxima and minima in the electrostatic potential surface (0.002 e/au isosurface) determined using a positive point charge in vacuum as a probe.
- S. Valiyaveetil, V. Enkelmann and K. Mullen, *J. Chem. Soc., Chem. Commun.*, 1994, 2097.
- Cambridge Structural Database ConQuest version 1.8.
- C. B. Aakeröy, N. Schultheiss and J. Desper, *Inorg. Chem.*, 2005, **44**, 4983.
- SMART v5.060, © 1997–1999, Bruker Analytical X-ray Systems, Madison, WI.
- SAINT v6.02, © 1997–1999, Bruker Analytical X-ray Systems, Madison, WI.
- SHELXTL v5.10, © 1997, Bruker Analytical X-ray Systems, Madison, WI.
- The relatively high *R*-value for this structure was due to thin and poorly diffracting crystals.
- (a) N. Shan, A. D. Bond and W. Jones, *New J. Chem.*, 2003, **2**, 365; (b) K. K. Arora and V. R. Pedireddi, *J. Org. Chem.*, 2003, **67**, 556; (c) T. Sugiyama, J. Meng and T. Matsuura, *J. Mol. Struct.*, 2002, **611**, 53; (d) N. Shan, E. Batchelor and W. Jones, *Tetrahedron Lett.*, 2002, **43**, 8721; (e) B. R. Bhogala and A. Nangia, *Cryst. Growth Des.*, 2002, **2**, 325; (f) M. J. Zaworotko, *Chem. Commun.*, 2001, 1.
- (a) K. Chinnakali, H.-K. Fun, S. Goswami, A. K. Mahapatra and G. D. Nigam, *Acta Crystallogr., Sect. C: Cryst. Struct. Commun.*, 1999, **C55**, 399; (b) S. Goswami, A. K. Mahapatra, K. Ghosh, G. D. Nigam, K. Chinnakali and H.-K. Fun, *Acta Crystallogr., Sect. C: Cryst. Struct. Commun.*, 1999, **C55**, 87; (c) D. E. Lynch, G. Smith, K. A. Byriel and C. H. L. Kennard, *Aust. J. Chem.*, 1998, **51**, 403; (d) G. Smith, J. M. Gentner, D. E. Lynch, K. A. Byriel and C. H. L. Kennard, *Aust. J. Chem.*, 1995, **48**, 1151.